Estimation of Clarinet Reed Parameters by Inverse Modelling

Chatziioannou, V., & Van Walstijn, M. (2012). Estimation of Clarinet Reed Parameters by Inverse Modelling. *Acta Acustica united with Acustica*, *98*(4), 629 – 639. https://doi.org/10.3813/AAA.918543

Published in:
Acta Acustica united with Acustica

Document Version:
Early version, also known as pre-print

Estimation of clarinet reed parameters by inverse modelling

Vasileios Chatziioannou
Institute of Musical Acoustics
University of Music and performing Arts, Vienna
Anton von Webern Platz 1, 1030 Vienna, Austria
chatziioannou@mdw.ac.at

Maarten van Walstijn
Sonic Arts Research Centre
Queen's University Belfast
BT7 1NN Belfast, Northern Ireland
m.vanwalstijn@qub.ac.uk

November 5, 2012

Abstract

Analysis of the acoustical functioning of musical instruments invariably involves the estimation of model parameters. The broad aim of this paper is to develop methods for estimation of clarinet reed parameters that are representative of actual playing conditions. This presents various challenges because of the difficulties of measuring the directly relevant variables without interfering with the control of the instrument. An inverse modelling approach is therefore proposed, in which the equations governing the sound generation mechanism of the clarinet are employed in an optimisation procedure to determine the reed parameters from the mouthpiece pressure and volume flow signals. The underlying physical model captures most of the reed dynamics and is simple enough to be used in an inversion process. The optimisation procedure is first tested by applying it to numerically synthesised signals, and then applied to mouthpiece signals acquired during notes blown by a human player. The proposed inverse modelling approach raises the possibility of revealing information about the way in which the embouchure-related reed parameters are controlled by the player, and also facilitates physics-based resynthesis of clarinet sounds.

1 Introduction

The physics of single-reed woodwind instruments has been studied throughout the past century. In 1929 Bouasse presented a series of observations on the functioning of woodwind instruments [1]. In later work, a mathematical framework for studying the oscillations of such instruments was developed [2, 3, 4, 5, 6], which provided the necessary basis for the formulation of full, predictive physical models (see, e.g. [7, 8]). Some uncertainties remain though, particularly regarding the complex fluid dynamics in the reed channel, and how this interacts with the reed motion [9, 10].

In most studies, the reed is modelled as a single-mass harmonic oscillator, which can be justified by considering that its dimensions are small compared to the wavelengths inside the instrument. Several researchers have provided estimations of the lumped parameters of such a simplified mechanical reed model. In 1969 Nederveen measured the compliance of the reed by observing its deformation in static experiments [6]. Worman [11] determined the effective stiffness, damping, and mass per unit area of an isolated reed experimentally and his results were adopted by many subsequent authors [12, 13, 14]. Another measurement of the reed stiffness was provided by Gilbert [15] and his

results were in agreement with the compliance measured by Nederveen. It is worthwhile noting that, apart from Worman, the above researchers used dry reeds, thus the estimations may not be representative of playing conditions. Moreover, the influence of the player's lip is often neglected, and the interaction with the mouthpiece lay was generally treated in a simplified way, by imposing a 'hard' beating condition.

The first published attempt to measure reed stiffness under actual playing conditions was made by Boutillon and Gibiat [16]. They derived the stiffness of a saxophone reed by establishing a balance between the reactive powers of the reed and the air-column. The obtained range of values was of the same order as that found by Nederveen and Gilbert. Gazengel [17] developed a model in which the reed-lay interaction is modelled by varying the lumped parameters within the reed cycle. The lumped parameter functions were deduced theoretically by considering a distributed interaction with the mouthpiece lay, using simplified geometries for both the reed and the mouthpiece. More recently it has been shown how the lumped reed model parameters can be estimated from a distributed model while considering a more realistic geometry of the system, also incorporating the lip influence [18]. In particular it has been demonstrated how the effective stiffness per unit area and the effective moving surface of the reed can be estimated as functions of the pressure difference across the reed. The notion of a variable stiffness in order to capture the nonlinear interaction of the reed with the mouthpiece lay was also suggested in an experimental study by Dalmont et al. [19].

In the present study a method is presented to estimate lumped reed model parameters from mouthpiece oscillations. The reed model is formulated using a constant stiffness, and the reed-lay interaction is instead modelled by means of a conditional repelling force, in a way similar to modelling of piano hammer-string interaction [20]. The objective behind this is to formulate a more simple reed model with relatively few parameters that nevertheless captures most of the dynamics of the reed-player-mouthpiece system, so that it can sufficiently adapt to experimental data. This model is then employed in an inverse modelling procedure which, given the pressure and flow signals in the mouthpiece, estimates the lumped reed parameters. When using signals measured during human player control of the instrument, the estimated parameters partly reflect the actions of the player. This raises the possibility of physics-based re-synthesis of clarinet sounds [21, 22], and also opens up a new way of investigating how players control the instrument in practice. In addition, the results of the inverse modelling approach can give new perspectives and insights into the validity and accuracy of the lumped reed model.

Studying the functioning and control of wind instruments using an inverse modelling approach has been attempted before, usually starting from a single pressure signal, which imposes fairly strong limitations on the inversion process. For example, investigations into the inversion of a trumpet model have shown that additional assumptions and constraints have to be applied in order to avoid problems of uniqueness and non-invertibility [23, 24]. Regarding the clarinet, several attempts have been made to identify the sound generation loop of a (simplified) clarinet using an artificial blowing setup [25, 26], but the employed sensing methods have not yet been demonstrated to be sufficiently accurate for subsequent parameter estimation. In order to avoid or reduce some of the problems encountered in these studies, this paper addresses the determination of clarinet reed parameters from two in-duct signals, namely the pressure and volume flow in the mouthpiece. For estimation from experimental data, the flow signal is difficult to measure directly, but can be inferred from pressure signals acquired in the instrument bore.

The paper is structured as follows: Starting from a brief discussion on recent distributed modelling results, the lumped formulation of the reed is reconsidered under the inverse modelling scope in section 2, and a full time-domain model of a simplified clarinet without toneholes is presented. The inversion of the model is discussed in section 3, including an analysis of the performance for numerically generated pressure and flow signals. Then in section 4, the results of applying the inversion to signals obtained under real playing conditions are presented and discussed. Finally, the conclusions are summarised in section 5.

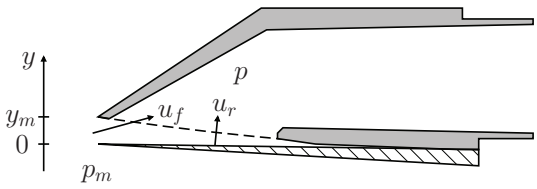

Figure 1: Schematic illustration of a clarinet mouthpiece. The mouthpiece tip displacement is denoted with y, the equilibrium opening with y_m, the flow in the reed channel with u_f, and the reed induced flow with u_r, while p and p_m represent the mouthpiece pressure and the mouth pressure, respectively.

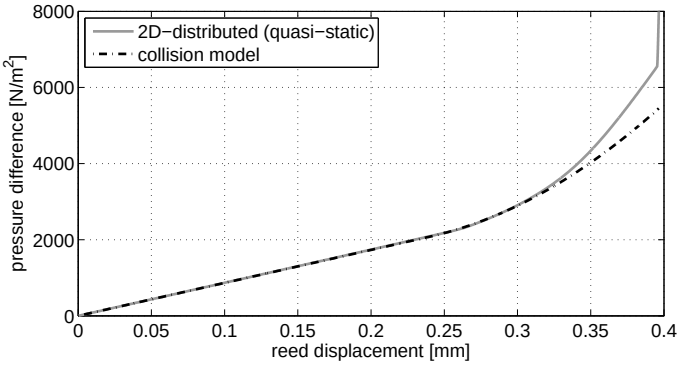

Figure 2: An example of (quasi-static) pressure difference versus reed tip displacement as computed with the distributed model (grey solid curve). The dashed curve indicates the lumped model approximation with equation (1). The reed tip touches the mouthpiece lay at $y = 0.4$mm.

2 Time-domain modelling

2.1 Distributed reed modelling results

Figure 1 shows a schematic depiction of a clarinet mouthpiece and the associated parameters. The mechanical response of the reed-mouthpiece system can be studied via numerical simulations with a distributed reed model. This allows bringing in the geometrical detail of the reed-mouthpiece system, and facilitates investigating the interaction between the reed and the mouthpiece lay. In several earlier studies, the reed has been modelled as a one-dimensional clamped bar [27, 28]; later refinements to this approach were made regarding the formulation of the lip-reed and the reed-lay interaction [29]. More recently, a two-dimensional distributed model of the reed has been developed [30] which also captures the torsional behaviour of the reed; details of the numerical formulation of this model can be found in [31, Chapter 3]. One of the main results that can be obtained with these simulations is the quasi-static mechanical behaviour of the reed. The solid grey curve in Figure 2 shows a typical example of plotting the pressure difference against the tip displacement from quasi-static numerical experiments with the 2-D reed model presented in [30]. The plot demonstrates that the reed behaves largely as a linear spring in the range of tip displacements in which there is little interaction between the reed and the lay. For larger displacements, the lay exerts additional contact forces on the reed, which 'bend' the curve upwards.

2.2 A lumped reed model

In previous publications, the relationship between pressure difference and reed tip displacement was used to deduce the stiffness per unit area as a (nonlinear) function of the pressure difference [18, 30]. In the current study, the reed stiffness is kept constant, and as in hammer-string modelling [20], the reed-lay interaction is modelled with a conditional contact force based on a power-law. For quasi-static reed motion, the reed tip motion is then governed by

$$k\,y + k_c\,(\lfloor y - y_c \rfloor)^\alpha = \Delta p, \tag{1}$$

where $\Delta p = p_m - p$ is the pressure difference across the reed, k is the effective reed stiffness per unit area, k_c and α are power-law constants, and y_c represents the displacement value above which the contact force becomes active, i.e.

$$\lfloor y - y_c \rfloor = \begin{cases} y - y_c & \text{if } y > y_c \\ 0, & \text{otherwise.} \end{cases} \tag{2}$$

A similar 'collision model' approach can be found in recent methods for synthesis-oriented time-domain modelling of reed woodwinds [32, 33]. The dashed line in Figure 2 shows the approximation of equation (1) to the distributed model result for $\alpha = 2$. The fit is not accurate for near-closure displacements, but in practice (when the reed behaves dynamically), the clarinet configurations we studied do not support the production of mouthpiece pressure signals larger than about 4400 N/m^2 (even

for blowing pressures that close the reed). Hence this discrepancy hardly influences the simulation results, and consequently has little bearing on the inversion process. Therefore $\alpha = 2$, which generally gives an excellent fit for the range of y-values just above y_c, was used in all computations.

A lumped reed model that also incorporates some reed dynamics may then be formulated by adding mass and damping to (1):

$$m\,\frac{d^2y}{dt^2} + m\,g\frac{dy}{dt} + k\,y + k_c\,(\lfloor y - y_c \rfloor)^\alpha = \Delta p, \quad (3)$$

where m is the effective reed mass and g is the damping per unit area; these reed parameters can in principle also be determined from distributed model simulation results [18].

2.3 The mouthpiece flow

As indicated in Figure 1, the flow into the mouthpiece consists of two components, namely the flow u_f through reed channel and the volume flux u_r induced by the reed motion:

$$u = u_r + u_f. \quad (4)$$

The flow through the reed channel is usually assumed to be governed by Bernoulli's law, considering the reed opening surface as a rectangle with sides λ and h [9, 19, 34]:

$$u_f = \lambda\,h\,\sqrt{\frac{2\Delta p}{\rho}}, \quad (5)$$

where $h = y_m - y$ is the reed opening, λ is the effective width of the reed and ρ the air density. This formulation is based on the simplifying assumption that both the side openings and the vena contracta effect result in a simple scaling of the flow through the reed channel. A more complex calculation of u_f is possible [34], on the basis of analytical formulations of the vena contracta effect [35], but its validity in dynamic regimes is difficult to establish.

The reed-induced flow u_r is commonly calculated as [6, 7]

$$u_r = S\,\frac{dy}{dt}, \quad (6)$$

where S is the effective reed surface. Although from distributed simulations S can be said to be varying with reed position, it has been shown that any variations in it do not significantly affect the model output [18, 31]. Therefore S is treated here as a constant.

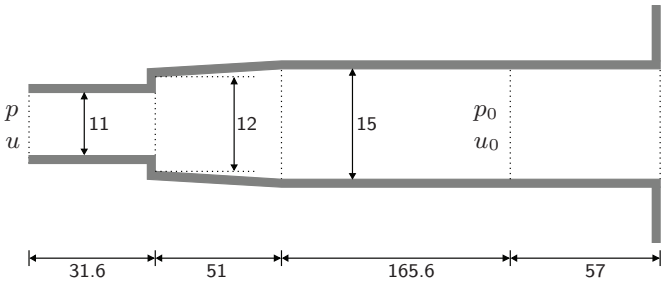

Figure 3: Schematic bore profile of the simplified clarinet bore (dimensions in mm).

2.4 Coupling to the bore

In order to simulate clarinet tones, the response of the bore must be modelled. Instead of using a realistic clarinet bore, the simplified configuration depicted in Figure 3 was employed, as it allows a much more reliable and accurate response prediction by theory than a bore with many toneholes and a flared bell. As will be seen in section 4, this is useful in providing an intermediate validation of the sensing approach when applied to measured signals.

Considering only plane waves, the response of the bore can be calculated via convolution of the forward-travelling pressure wave p^+ at the mouthpiece entry with the bore reflection function [14]:

$$p^- = r_f * p^+, \quad (7)$$

where p^- is the returning wave. The relationship with the mouthpiece flow is

$$Z_0\,u = p^+ - p^-, \quad (8)$$

where Z_0 is the characteristic impedance at the mouthpiece entry. Digital waveguide modelling [36, 37] was employed to pre-compute the bore reflection function r_f. This requires first constructing an axially symmetric representation of the instrument bore and mouthpiece. The main bore of the instrument is modelled as a straight cylinder and - following [37] - the mouthpiece is modelled as a cylindrical plus a conical section (see Figure 3 for dimensions). In order to determine the dimensions, a 3-D model of the interior shape of an actual mouthpiece was generated (see Figure 4) by 3-D scanning of a silicone cast, using the mouthpiece as a mould. The dimensions of the cylindrical part of the model are taken to have the same volume as the complex-shaped interior shape of the first part

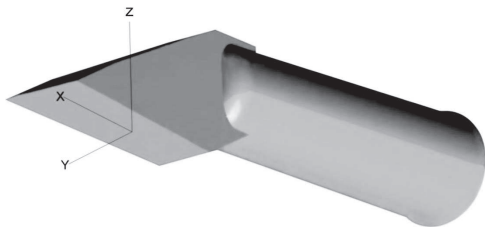

Figure 4: Model of the interior of a clarinet mouthpiece.

of the actual mouthpiece, whereas the dimensions of the conical part match the corresponding section of the actual mouthpiece.

A method to numerically solve the complete coupled system is given in Appendix A. Exciting the system with a constant blowing pressure p_m and using the lumped model parameters shown on the first column of Table 1 yields the pressure and flow signals in the mouthpiece depicted in Figure 5. These signals, which were generated using a 100 kHz sample rate, are used in the next section as the target signals of an inverse modelling method.

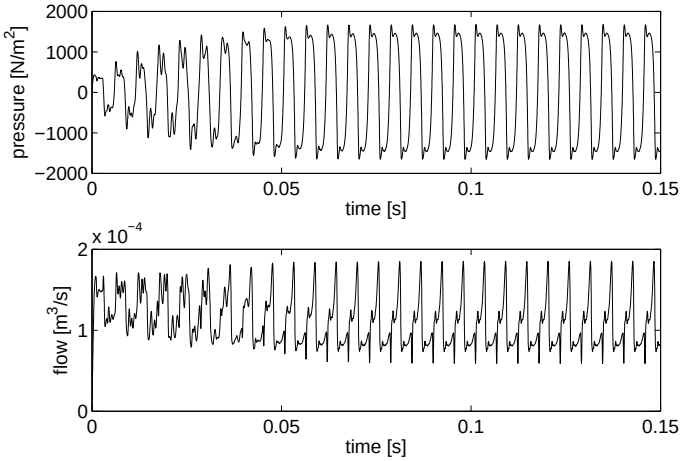

Figure 5: Pressure (top) and flow (bottom) signals in the mouthpiece, calculated using the parameters in the first column of Table 1.

3 Inverse modelling

Starting from the assumption that the pressure and flow signals in the mouthpiece are known, the aim is now to reverse the modelling direction, i.e. to estimate the physical model parameters from the signals. At first glance, it may look possible to design an optimisation method that finds the model parameters that minimise an objective function in a least square error sense. While such a method is indeed used in this study, initial attempts immediately revealed that the search space for this problem contains many local minima and spurious solutions, and that for the optimisation to be successful, a rather good initial guess is required. The strategy taken here is therefore to split the procedure into two optimisation stages, which will be referred to as step 1 and step 2 (see Figure 6). The first step is based on simplifying the equations that govern the reed motion, which allows formulating a closed-form expression that relates the pressure and flow signals in the mouthpiece. This step produces a first estimate of a reduced set of parameters, which then form a part of a parameter set that can be used as a suitable initial guess for the second optimisation step, which really aims to find a close match between the synthesis signals and the target signals. Convergence to spurious solutions that do not lie in the physical range of the model parameters is avoided this way.

3.1 First optimisation step

In the first step only a rough estimation of a parameter set is aimed for, which if used for resynthesis produces signals that are to some extent similar to the target signals. The highest priority in this step is not accuracy, but robustness. This can be achieved by simplifying the model equations somewhat, thus optimising a smaller parameter set. Aiming solely at the steady-state part of the signal, where dynamic effects are relatively small (see, for example, Figures 4 and 5 in [34]), a good way to simplify the model is to neglect reed damping and inertia. Another aspect that is temporarily disregarded is the reed-lay interaction. With those simplifying assumptions the reed motion is proportional to the pressure difference:

$$y = \frac{\Delta p}{k} = \frac{p_m - p}{k}. \tag{9}$$

Starting from (4), (5), and (6), and now considering also negative pressure differences, the total flow into the mouthpiece can be written as a function

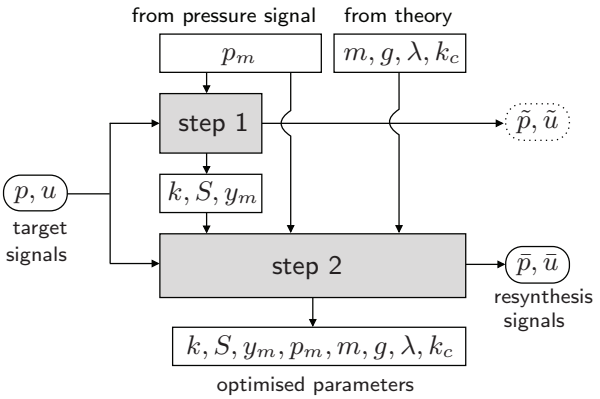

Figure 6: Two-step optimisation routine. The target signals are fed into the first optimisation step to estimate a parameter set. This set along with theoretical values for the remaining model parameters is the starting point for the second optimisation step. The parameters estimated in the two steps can be used for resynthesis of the pressure and flow signals.

of pressure only:

$$
\begin{aligned}
u &= \underbrace{\sigma\,\lambda\,\lfloor y_m - y \rfloor \sqrt{\frac{2\,|p_m - p|}{\rho}}}_{u_f} + \underbrace{S\,\frac{dy}{dt}}_{u_r} \\
&\overset{(9)}{=} -\frac{\sigma\lambda}{k}\sqrt{\frac{2}{\rho}}\,|p_m - p|^{\frac{3}{2}} + \sigma y_m \lambda \sqrt{\frac{2}{\rho}}\,|p_m - p|^{\frac{1}{2}} \\
&\quad - \frac{S}{k}\frac{dp}{dt} \\
&= \sigma\sqrt{\frac{2}{\rho}}\left(c_1\,|p_m - p|^{\frac{3}{2}} + c_2\,|p_m - p|^{\frac{1}{2}}\right) + c_3\frac{dp}{dt}, \\
&= c_1 d_1 + c_2 d_2 + c_3 d_3,
\end{aligned}
\tag{10}
$$

where σ is the sign of $(p_m - p)$ and

$$
\begin{cases} c_1 = -\lambda/k \\ c_2 = y_m\lambda \\ c_3 = -S/k \end{cases}
\Rightarrow
\begin{cases} k = -\lambda/c_1 \\ y_m = c_2/\lambda \\ S = \lambda\, c_3/c_1 \end{cases},
\tag{11}
$$

and where we have the three signals

$$
d_1 = q\,|p_m - p|^{\frac{3}{2}}, d_2 = q\,|p_m - p|^{\frac{1}{2}}, d_3 = \frac{dp}{dt}, \tag{12}
$$

where $q = \sigma\sqrt{2/\rho}$. A characteristic feature of this approach is that the flow u_r in equation (10) brings into effect the derivative of the pressure with respect to time (dp/dt). This gives a simple tool for distinguishing between the opening and closing phases of the reed motion, i.e. the two branches

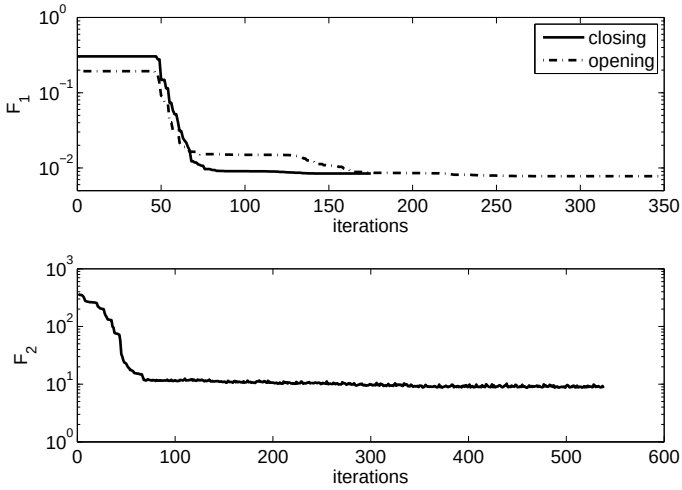

Figure 7: Evolution of the objective functions F_1 (top) and F_2 (bottom).

that appear if we plot flow against pressure difference (see Figure 8). Hence step 1 is run separately for two parts of the data; once for the opening state $(dp/dt > 0)$ and once for the closing state $(dp/dt < 0)$ of the reed motion; although usable results can be estimated from either branch, the results used for step 2 are obtained from the closing branch estimates.

Equation (10) relates the pressure and the flow inside the mouthpiece, which are assumed known in this context. For the mouth pressure p_m a reasonably good estimate can be obtained directly from the pressure signal vector $\mathbf{p}$ as $p_m = \max|\mathbf{p}|$. The air density ρ is also assumed to be known, so the task is to find the three coefficients c_1, c_2, and c_3. To this purpose, the square of an L^2 norm is used as an objective function, namely

$$
F_1 = ||(\mathbf{u} - \tilde{\mathbf{u}})||_2^2, \tag{13}
$$

in order to minimise the difference between the target flow signal vector $\mathbf{u}$ and the flow signal vector $\tilde{\mathbf{u}}$ calculated with (10). By substituting (10) into (13) and taking the second-order partial derivatives of the objective function F_1 with respect to c_i (i = 1,2,3), one obtains

$$
\frac{\partial^2 F_1}{\partial c_i^2} = 2\sum_{n=1}^{N} d_i^2(nT), \tag{14}
$$

where n indexes the sample in the vector $\tilde{\mathbf{u}}$ and N is the vector length. Hence the second derivatives of F_1 are guaranteed to be positive, thus the objective

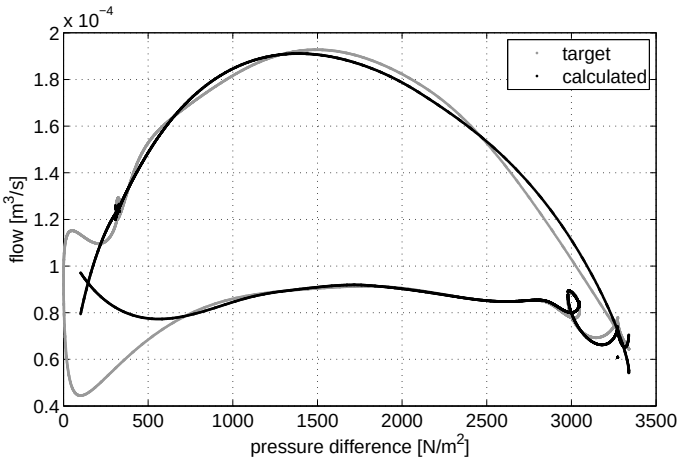

Figure 8: Flow into the mouthpiece over pressure difference, for the original model (grey) and as calculated by equation (10) using the estimated parameters (black). Note that the closing and opening phase are calculated separately, and plotted as separate curves (they cross at about $\Delta p = 150$ N/m^2).

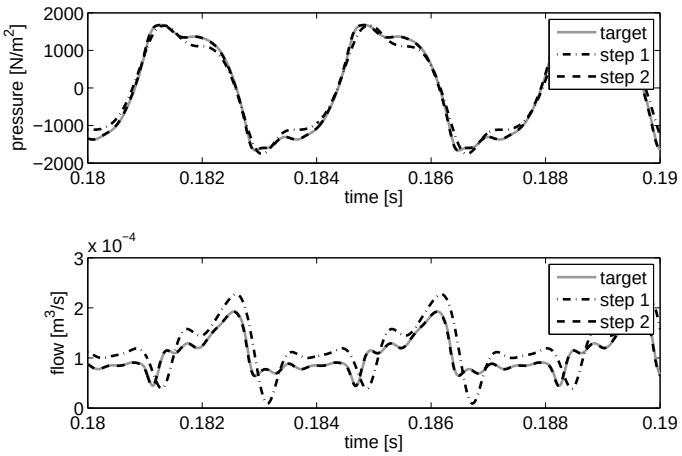

Figure 9: Pressure (top) and flow (bottom) signals in the mouthpiece as synthesised using the estimated parameters after the first and the second optimisation steps, compared to the target signals (original model, grey solid).

function is concave, which enables a robust optimisation with standard methods; the Nelder-Mead simplex method [38] proved both efficient and sufficient in terms of robustness in this case. This procedure yields an optimised set of three coefficients, but these are related to four physical parameters (λ, k, y_m and S), so the actual physical parameters cannot be determined with (11) without further information. To address this redundancy problem, λ is simply set to the actual value of the geometrical reed width and its optimisation is only carried out during the second step. The optimisation method converged after 175 iterations for the closing and after 348 iterations for the opening branch (with the termination criterion being a relative change in all the estimated parameters smaller than 1%). The evolution of the objective function is shown in the upper plot of Figure 7.

One way to evaluate the obtained results of this first estimation of the physical model parameters is to compare the target flow with the flow as calculated with (10) using the set of the estimated parameters. These signals are plotted in Figure 8 over the pressure difference across the reed. A second way of comparing is to feed the optimised parameters (which are listed in the third column of Table 1) to the time-domain model and compare the resulting pressure and flow in the mouthpiece (the 'resynthesised signals') to the target signals synthesised using the original model (see Figure 9).

In summary, step 1 is successful in that the estimated parameters enable the synthesis of sustained oscillatory clarinet signals that, to a certain degree, resemble the target signals. This was found to be the case for a wide range of signals generated using different bore configurations and excitation parameters, and also when some noise was added [39].

3.2 Second optimisation step

For the second optimisation step, we use as objective function the L^2 norm of the difference between the target and the resynthesised pressure signals at steady state,

$$F_2 = ||\mathbf{p} - \bar{\mathbf{p}}||_2 \,, \tag{15}$$

and employ the Rosenbrock method [40] to locate the corresponding optimum set of parameters. Comparing the pressure rather than the flow signals, as in equation (13), ensures better convergence properties. The Rosenbrock algorithm is a direct search method, that can go through an M-dimensional search space. Starting with a set of M orthogonal directions, the algorithm moves towards those directions that reduce the value of the objective function (for minimisation problems) and then it changes the directions to a new orthogonal set, more likely to yield better results. It has the advantage that by changing the set of the search directions, it can adapt to narrow 'valleys' that may appear in the search-space. In addi-

tion, by expanding the motion towards successful directions and reducing that towards unsuccessful ones, it has the ability to avoid getting trapped within regions of local minima. The choice of the Rosenbrock method stems from the fact that, even though it is computationally expensive, it is robust for high dimensional problems, as long as a good starting point (that is given by the first optimisation step) is available, whereas the Nelder-Mead simplex method turns out to fail when the dimensions of the problem increase [41].

In our application, we run the clarinet simulation after each parameter search within the Rosenbrock algorithm, to synthesise the pressure signal in the mouthpiece and compare it to the target one. In contrast to the first optimisation step, it is now possible to include in the model almost all the physical model parameters, namely k, S, y_m, p_m, mass m, damping g, effective width λ and collision coefficient k_c; the only parameter that is not optimised is y_c, which is assumed not to deviate much from the value $y_c = 0.24$ mm, as taken from the distributed model result in Figure 2, and is set to that value. The reason for this is that when y_c is also optimised, step 2 is far more likely to converge to spurious solutions.

Since the target signals are governed by the same model that is used in the inversion, the parameters can be recovered, i.e. the estimated parameters are nearly identical to the original model parameters upon convergence. For the target signals calculated in section 2.4, using a 50 ms signal window, the algorithm converged (to a threshold relative error set to 0.03%) after 538 iterations. The resulting evolution of the objective function is shown in the lower plot of Figure 7. Applying the algorithm to more data sets showed that the rapid improvement in the first few iterations followed by a slower convergence period is typical for step 2. A comparison between the target signals and the resynthesised pressure and flow in the mouthpiece can been seen in Figure 9. The estimated parameters from both optimisation steps are listed in Table 1 .

Table 1: Theoretical (target) parameters and estimated parameters after the two optimisation steps.

parameter	theoretical	step 1	step 2
k [Pa/m]	8.66e6	8.72e6	8.68e6
S [m^2]	7.62e-5	9.66e-5	7.65e-5
y_m [m]	4e-4	4.4e-4	3.99e-4
p_m [Pa]	1800	1683	1799
λ [m]	0.013	—	0.0129
m [kg/m^2]	0.05	—	0.050
g [1/s]	3000	—	2979
k_c [Pa/m^2]	8.23e10	—	8.35e10

4 Application to measured signals

The next step is to investigate how the methodology works for measured signals. The main objective within the scope of this paper is to test whether the approach still works without problems in that scenario, i.e. whether physically plausible parameters are estimated and whether the signals can be reasonably accurately resynthesised. The starting point in this investigation is a set of signals measured at a specific point in the bore of a simplified clarinet (geometry shown in Figure 3) under playing conditions. The details of the employed technique to measure these signals - the basics of which are explained in [42] - are outside the scope of this paper, and will be published in separate articles.

In the experiments, the player generated a sustained note of about 4 seconds. The signals captured by three microphones embedded in the side wall of the main cylindrical bore (spaced 2 cm apart) were then processed using an adaptive filtering approach in order to derive the pressure and the flow at the reference plane. This method involves estimation of the parameters that model the transfer function between the microphones, and adapts to time-varying playing conditions (including the mean flow in the bore). All signals were acquired and processed using a 100 kHz sample rate.

4.1 Signal Translation

Given the pressure (p_0) and volume flow (u_0) at the reference plane (see Figure 3), the first step in the processing chain is to translate these to the corresponding pressure (p) and flow (u) at the mouthpiece entry. This can be achieved with classical transmission-line theory using ABCD matrices [43]. That is, in the frequency-domain the following calculation is performed

$$\begin{bmatrix} P \\ U \end{bmatrix} = \begin{bmatrix} A & B \\ C & D \end{bmatrix} \begin{bmatrix} P_0 \\ U_0 \end{bmatrix}, \qquad (16)$$

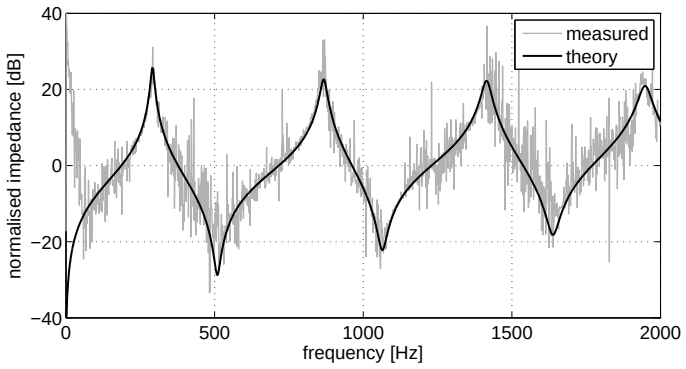

Figure 10: Theoretical and experimental input impedance of the flanged pipe used for the experiments.

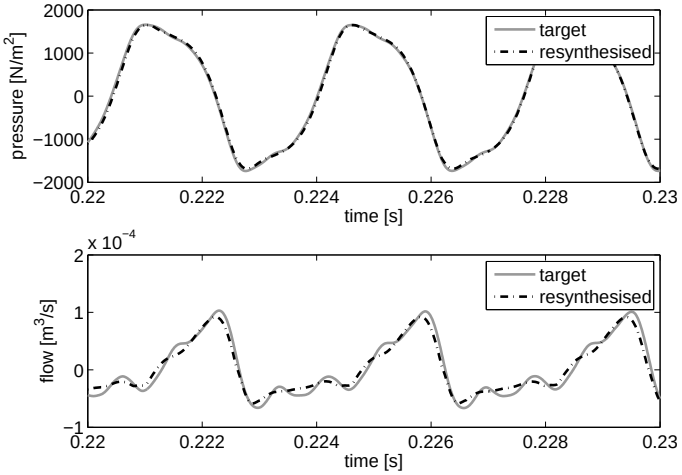

Figure 11: Pressure (top) and flow (bottom) signal resyntesised after step 2, compared to the measured target signals (grey-solid). The flow signals do not contain the mean flow component.

for a discrete set of frequencies, and FFTs are used to transform between the time and the frequency domain. The matrix elements are calculated from the geometry and the estimated air constants [43]. Linear-phase low-pass FIR filtering [44] with a 7.25 kHz cut-off is applied to both signals in order to remove high frequency errors that arise from the singularities inherent to the multiple-microphone wave separation method.

The translation procedure can be validated to some extent by comparing the theoretical (normalised) input impedance of the instrument - also calculated using transmission-line theory - to the frequency-domain ratio $P/(Z_0U)$ (see Figure 10). The measured data is contaminated by noise (the level of which cannot be reduced by averaging or using longer signals since only short-time blocks can be assumed to have constant conditions), but the global fit to theory is good. A flanged end was used (see Figure 3), the termination impedance of which is given in [45]. An unflanged end was tried as well, but this created relatively large discrepancies between the theoretical and experimental impedance curves, which is due to not having a termination impedance description of similar prediction accuracy available for an unflanged open pipe. Note that since the input impedance represents the same information as the bore reflection function r_f, a good match here is crucial, as otherwise step 2 of the optimisation routine (that relies on the accuracy of r_f) would fail.

4.2 Optimisation

The inversion algorithm is now applied to the experimentally determined mouthpiece pressure and flow signals. In order to ensure sufficiently constant conditions (i.e. all parameters involved can be assumed constant over the window period), a short window of 20 ms was used.

A couple of issues have to be dealt with before proceeding with the optimisation. Firstly, the measured signals are zero-mean, while the time-domain clarinet model produces a flow signal that contains the mean flow component. Hence a high-pass filtering routine is applied to the output of the model, so that the estimated and measured flow can be directly compared. Secondly, a problem that has to be tackled before proceeding with step 2 is that the signals obtained from the measurements and the ones resynthesised using the lumped model will now not be in phase. This was not the case in section 3.2, since both signals were generated numerically, using the same excitation model. Therefore a simple synchronisation procedure is now built into step 2.

The resynthesis signals resulting from applying the complete optimisation routine are shown in Figure 11. As can be seen, the pressure signal is resynthesised accurately. With numerically synthesised target signals, the match in the flow signals would then automatically also be good, since the forward and the inverse procedure use exactly the same physical model. This is however not the case for measured target signals. As can be seen from the lower plot of Figure 11, the flow match is globally good, but small deviations in the waveform

remain, and are not diminishing with more step 2 iterations. Explaining the causes of these small deviations from the available data is difficult, but it is nevertheless useful to make an initial assessment by considering the different stages in the processing chain at which errors may arise:

(A) errors introduced at the measurement stage, in particular due to non-perfect calibration,

(B) errors introduced in translating the measured signals (p_0, u_0) to the mouthpiece signals (p, u), in particular errors caused by using a simplified geometry of the mouthpiece,

(C) errors due to the simplified reed dynamics,

(D) errors introduced by having simplified the fluid dynamics in the mouthpiece and the reed channel to a quasi-static approximation.

The fairly good match in input impedance (see Figure (10)) suggests that the errors under (A) and (B) are relatively small. Regarding (C), the oscillatory motion per cycle in the measured flow signal might indicate some form of reed resonance which the inversion procedure does not manage to fully adapt to. Regarding (D), it is not yet understood to what extent equation (5) is valid for dynamic regimes, during which the "vena contracta" factor at low Δp regimes may not be constant [10]; further uncertainties exist regarding the effect of turbulence and how the lateral flow into the mouthpiece can affect the mouthpiece flow. To come to more conclusive explanations, these issues would first have to be investigated separately (where possible), which in turn would require experiments in which the conditions can be controlled more precisely.

All of the estimated parameters (see Table 2) are physically feasible. In fact most parameters are not too far off the corresponding value found in the literature (see theoretical values in Table 1), apart from the damping per unit area g, which in this case was considerably smaller.

Table 2: Estimated parameters extracted from the measured signals after the two optimisation steps.

parameter	step 1	step 2
k [Pa/m]	1.49e7	1.24e7
S [m^2]	2.1e-4	1.77e-4
y_m [m]	2.49e-4	2.55e-4
p_m [Pa]	1658	1671
λ [m]	—	0.012
m [kg/m^2]	—	0.056
g [1/s]	—	453
k_c [Pa/m^2]	—	3.7e11

5 Conclusions

In this paper an inversion procedure has been presented which, given pressure and flow signals in a clarinet mouthpiece, can estimate physically meaningful parameters. The procedure optimises the parameters of a simplified lumped model that aims to capture most of the dynamics of the reed-mouthpiece system. In this model, the (non-linear) interaction of the reed with the mouthpiece lay is modelled using a repelling force when the reed starts being in contact with the lay (and before it closes completely). This allows the use of just two constant parameters, namely the effective stiffness per unit area of the reed and the beating stiffness coefficient, in order to model the reed-lay interaction. The use of two constant parameters, rather then a generally varying parameter (e.g. $k(\Delta p)$) or the use of 'hard beating' is one of several modelling choices made in order to facilitate robust inversion.

The optimisation procedure consists of two steps, where the first step - that relies on several simplifications - serves as a robust initial-guess provider for the fine-tuning second step. For numerically generated target signals, the inversion procedure recovers the model parameters, indicating the correctness of the method, and extensive testing with different signal sets has demonstrated its robustness. For measured target signals, there is no reference for the estimated parameters, but as shown in section 4 the procedure can successfully resynthesise the pressure and flow signals, and the optimised parameters all lie in a physically feasible range. Any small discrepancies display themselves mainly in the flow signal. When applied to transient oscillations, the presented method does not give consistent results; in particular the first optimisation step appears to require a time-invariant pressure-flow relationship in a data window of sufficient length in order to systematically converge to physically plausible results.

In summary, the results indicate that the pro-

posed inversion approach is a promising new way of estimating reed parameters from player-controlled woodwind oscillations. Improvements would be possible if the parameter y_c could also be optimised, and/or if a refinement can be made in the descriptions of the reed motion and the fluid dynamics in the mouthpiece. Both of these steps would probably require the measurement of a signal that represents the effective reed opening. An interesting future research direction may therefore be to apply the method to oscillations generated with an artificial blowing machine, which would allow observing the relevant phenomena.

Acknowledgements

This work was supported by the Engineering and Physical Sciences Research Council (UK), Grant No EP/D074983/1. The authors are grateful to Giovanni de Sanctis (Queen's University Belfast) for providing the measurement signals acquired under playing conditions, as well as for further fruitful discussions and advice.

A Solving the coupled system

The system of equations to be solved is described by equations (3 - 8). This is done numerically using finite difference approximations of any of the derivative terms in these equations, leading to the following set of discrete-time equations:

$$\begin{aligned} y(n+1) &= a_1 y(n) + a_2 y(n-1) + \\ &\quad b_1 \Delta p(n) + a_3 \left(\lfloor y(n) - y_c \rfloor\right)^q, && \text{(A.1)} \\ h(n+1) &= y_m - y(n+1), && \text{(A.2)} \\ u_r(n+1) &= S\,\frac{y(n+1)-y(n)}{\Delta T}, && \text{(A.3)} \\ p^-(n+1) &= \sum_{i=0}^{N_f} r_f(i)\, p^+(n-i), && \text{(A.4)} \\ u_f(n+1) &= \lambda\, h(n+1)\sqrt{\frac{2\Delta p(n+1)}{\rho}}, && \text{(A.5)} \end{aligned}$$

$$\begin{aligned} u(n+1) &= u_r(n+1) + u_f(n+1), && \text{(A.6)} \\ Z_0 u(n+1) &= p^+(n+1) - p^-(n+1), && \text{(A.7)} \\ p(n+1) &= p^+(n+1) + p^-(n+1), && \text{(A.8)} \\ \Delta p(n+1) &= p_m(n+1) - p(n+1), && \text{(A.9)} \end{aligned}$$

with equation (A.1) yielding the displacement at the next time step ($y(n+1)$) knowing the current values $\Delta p(n)$ and $y(n)$ and the previous value $y(n-1)$, where time is discretised as $t = n\Delta T$. The coefficients a_1, a_2, a_3 and b_1 were calculated here using centered difference operators. The numerical dispersion and attenuation introduced in these approximations is negligible in the frequency range of interest due to the use of a high (100 kHz) sample rate, and this also ensures that the relevant stability bounds are satisfied for any physically feasible parameters. From the displacement at time $n+1$ it is possible to calculate the reed opening h and the reed induced flow u_r. However, for the computation of u_f equation(A.5) needs to be written as

$$\Delta p = \mathrm{sign}(\Delta p)\frac{\rho}{2(\lambda h)^2} u_f^2. \qquad \text{(A.10)}$$

Substituting

$$\Delta p = p_m - p = p_m - 2p^- - Z_0 u_f - Z_0 u_r, \qquad \text{(A.11)}$$

we get

$$\begin{aligned} &\mathrm{sign}(\Delta p) u_f^2 + 2\underbrace{\frac{(\lambda h)^2 Z_0}{\rho}}_{\Lambda} u_f \\ &\qquad + \underbrace{\frac{2(\lambda h)^2}{\rho}(2p^- + Z_0 u_r - p_m)}_{\Gamma} = 0 \\ &\Rightarrow \mathrm{sign}(\Delta p) u_f^2 + 2\Lambda u_f + \Gamma = 0, \end{aligned} \qquad \text{(A.12)}$$

with h, u_r, p_m and p^- all evaluated at the next time step ($t = (n+1)\Delta t$). There are two cases to consider depending on the sign of Δp.

- If $\mathrm{sign}(\Delta p) = 1$:

$$u_f = \frac{-2\Lambda \pm \sqrt{4\Lambda^2 - 4\Gamma}}{2} = -\Lambda \pm \sqrt{\Lambda^2 - \Gamma} \qquad \text{(A.13)}$$

  and since $\Delta p \geq 0 \Rightarrow u_f \geq 0$ then

$$\sqrt{\Lambda^2 - \Gamma} \geq \Lambda \Rightarrow \underline{\Gamma \leq 0} \qquad \text{(A.14)}$$

- If $\mathrm{sign}(\Delta p) = -1$:

$$u_f = \frac{-2\Lambda \pm \sqrt{4\Lambda^2 + 4\Gamma}}{-2} = -\Lambda \pm \sqrt{\Lambda^2 + \Gamma} \qquad \text{(A.15)}$$

  and since $\Delta p < 0 \Rightarrow u_f < 0$ then

$$\sqrt{\Lambda^2 + \Gamma} > \Lambda \Rightarrow \underline{\Gamma > 0}. \qquad \text{(A.16)}$$

Wrapping up both cases, u_f can be directly calculated by first determining the sign of Γ and then carrying out the following operation

$$\begin{cases} \text{if } \Gamma(n+1) \leq 0 \text{ then} \\ u_f(n+1) = -\Lambda(n+1) + \sqrt{\Lambda(n+1)^2 - \Gamma(n+1)} \\ \\ \text{if } \Gamma(n+1) > 0 \text{ then} \\ u_f(n+1) = \Lambda(n+1) - \sqrt{\Lambda(n+1)^2 + \Gamma(n+1)}. \end{cases} \tag{A.17}$$

Next the total flow trough the reed is calculated with A.6; the calculation of $\Gamma(n+1)$ requires knowledge of $p^-(n+1)$, which is obtained by the convolution in equation (A.4), where N_f is the length of r_f. Finally, the outgoing pressure wave is calculated using (A.7), and the result is then used to update the mouthpiece pressure $p(n+1)$ with (A.8) and the pressure difference $\Delta p(n+1)$ with (A.9).

References

[1] H. Bouasse. *Instruments à vent, volume 1.* Librairie Delagrave, Paris, 1929.

[2] J. Backus. Vibrations of the reed and air column in the clarinet. *Journal of the Acoustical Society of America*, 33(6):806–809, 1961.

[3] J. Backus. Small-vibration theory of the clarinet. *Journal of the Acoustical Society of America*, 35(3):305–313, 1963.

[4] T.A. Wilson and G.S. Beavers. Operating modes of the clarinet. *Journal of the Acoustical Society of America*, 56(2):653–658, 1974.

[5] A.H. Benade and D.J. Gans. Sound production in wind instruments. *Annals of the New York Academy of Sciences*, 155(1):247–263, 1968.

[6] C.J. Nederveen. *Acoustical Aspects of Woodwind Instruments.* Frits Knuf, Amsterdam, 1969.

[7] J. Gilbert, J. Kergomard, and E. Ngoya. Calculation of the steady-state oscillations of a clarinet using the harmonic balance technique. *Journal of the Acoustical Society of America*, 86(1):35–41, 1989.

[8] B. Gazengel, J. Gilbert, and N. Amir. Time domain simulation of single reed wind instrument. From the measured input impedance to the synthesis signal. Where are the traps? *Acta Acustica*, 3:445–472, 1995.

[9] A. Hirschberg, J. Gilbert, A.P.J. Wijnands, and A.M.C. Valkering. Musical aero-acoustics of the clarinet. *Journal De Physique IV*, C5:559–568, 1995.

[10] A.R. da Silva, G.P. Scavone, and M. van Walstijn. Numerical simulations of fluid-structure interactions in single-reed mouthpieces. *Journal of the Acoustical Society of America*, 120:1798–1810, 2007.

[11] W.E. Worman. *Self-Sustained Nonlinear Oscillations of Medium Amplitude in Clarinet-Like Systems.* PhD thesis, Case Western Reserve University, 1971.

[12] S.C. Thompson. The effect of the reed resonance on woodwind tone production. *Journal of the Acoustical Society of America*, 66(5):1299–1307, 1979.

[13] N.H. Fletcher. Excitation mechanisms in woodwind and brass instruments. *Acustica*, 43:63–72, 1979.

[14] R.T. Schumacher. Ab intio calculations of the oscillations of a clarinet. *Acustica*, 48(2):71–85, 1981.

[15] J. Gilbert. *Etude des instruments de musique à anche simple: extension de la méthode d'équilibrage harmonique, rôle de l'inharmonicité des résonances, mesure des grandeurs d'entrée.* PhD thesis, Université du Mans, Le Mans, France, 2002.

[16] X. Boutillon and V. Gibiat. Evaluation of the acoustical stiffness of saxophone reeds under playing conditions by using the reactive power approach. *Journal of the Acoustical Society of America*, 100(2):1178–1189, 1996.

[17] B. Gazengel. *Caractérisation objective de la qualité de justesse, de timbre et d'émission des instruments à vent à anche simple.* PhD thesis, Université du Maine, Le Mans, France, 1994.

[18] M. van Walstijn and F. Avanzini. Modelling the mechanical response of the reed-mouthpiece-lip system of a clarinet. Part II. A lumped model appproximation. *Acustica*, 93(1):435–446, 2007.

[19] J.P. Dalmont, J. Gilbert, and S. Ollivier. Nonlinear characteristics of single-reed instruments: Quasistatic volume flow and reed opening measurements. *Journal of the Acoustical Society of America*, 114(4):2253–2262, 2003.

[20] D.E. Hall. Piano string excitation. VI: Nonlinear modeling. *Journal of the Acoustical Society of America*, 92(1):95–105, 1992.

[21] M. van Walstijn and G. De Sanctis. Towards physics-based re-synthesis of woodwind tones. In *International Congress on Acoustics (ICA 2007), Madrid, Spain*, 2007.

[22] M. Sterling, Xiaoxiao Dong, and M. Bocko. Representation of solo clarinet music by physical modeling synthesis. In *Acoustics, Speech and Signal Processing, 2008. ICASSP 2008. IEEE International Conference on*, pages 129 –132, 2008.

[23] T. Hélie, C. Vergez, J. Lévine, and X. Rodet. Inversion of a physical model of a trumpet. In *38th Conference on Decision and Control*, Phoenix, Arizona, 1999.

[24] W. D'haes and X. Rodet. A new estimation technique for determining the control parameters of a physical model of a trumpet. In *6th International Conference on Digital Audio Effects (DAFx03), London, England*, 2003.

[25] G. P. Scavone. *An Acoustic Analysis of Single-Reed Woodwind Instruments with an Emphasis on Design and Performance Issues and Digital Waveguide Modeling Techniques*. PhD thesis, Music Dept., Stanford University, 1997. (Chapter 4, pp 172 – 195).

[26] T. Smyth and J. Abel. Estimating the reed pulse from clarinet recordings. In *International Computer Music Conference*, Montreal, 2009.

[27] S.E. Stewart and W.J. Strong. Functional model of a simplifed clarinet. *Journal of the Acoustical Society of America*, 68(1):109–120, 1980.

[28] S.D. Sommerfeldt and W.J. Strong. Simulation of a player-clarinet system. *Journal of the Acoustical Society of America*, 82(5):1908–1918, 1988.

[29] F. Avanzini and M. van Walstijn. Modelling the mechanical response of the reed-mouthpiece-lip system of a clarinet. Part I. A one-dimensional distributed model. *Acustica*, 90(1):537–547, 2004.

[30] V. Chatziioannou and M. van Walstijn. Reed vibration modelling for woodwind instruments using a two-dimensional finite difference method approach. In *International Symposium on Musical Acoustics*, Barcelona, 2007.

[31] V. Chatziioannou. *Forward and inverse modelling of single-reed woodwind instruments with application to digital sound synthesis*. PhD thesis, Queens University Belfast, School of Electronics, Electrical Engineering and Computer Science, Belfast, Northern Ireland, 2010.

[32] S. Bilbao. *Numerical Sound Synthesis*. John Wiley and Sons, 2009.

[33] S. Bilbao. Direct simulation of reed wind instruments. *Computer Music Journal*, 33(4):43–55, 2009.

[34] V. Chatziioannou and M. van Walstijn. A refined physical model of the clarinet using a variable air jet height. In *The 3rd International Symposium on Communications, Control and Signal Processing (ISCCSP)*, Malta, 2008.

[35] J. van Zon, A. Hirschberg, J. Gilbert, and A.P.J. Wijnands. Flow through the reed channel of a single reed music instrument. *Colloque de Phusique*, C2:821–824, 1990.

[36] J.O. Smith. Physical modeling using digital waveguides. *Computer Music Journal*, 16(4):74–91, 1992.

[37] M. van Walstijn and M. Campbell. Discrete-time modeling of woodwind instrument bores using wave variables. *Journal of the Acoustical Society of America*, 113(1):575–585, 2003.

[38] J.A. Nelder and R. Mead. A simplex method for function minimization. *The Computer Journal*, 7:308–313, 1964.

[39] V. Chatziioannou and M. van Walstijn. Extraction of lumped clarinet reed model parameters from numerically synthesised sound. In *Acoustics '08*, Paris, 2008.

[40] H.H. Rosenbrock. An automatic method for finding the greatest or least value of a function. *The Computer Journal*, 3:175–184, 1960.

[41] V. Torczon. *Multi-Directional Search: A Direct Search Algorithm for Parallel Machines*. PhD thesis, Department of Mathematical Sciences, Rice University, Houston, Texas, 1989.

[42] G. De Sanctis and M. van Walstijn. A frequency domain adaptive algorithm for wave separation. In *12th Int. Conference on Digital Audio Effects (DAFx-09)*, Como, Italy, 2009.

[43] D.H. Keefe. Woodwind air column models. *Journal of the Acoustical Society of America*, 88(1):35–51, 1990.

[44] J.G. Proakis and D.G. Manolakis. *Digital Signal Processing: Principles, Algorithms, and Applications*. MacMillan, New York, 1992.

[45] N. Fletcher and T. Rossing. *The Physics of Musical Instruments*. Springer, New York, 1998. 2nd edition.